Vol 12 No 9, September 2003
1009-1963/2003/12(09)/1011-05

Chinese Physics

© 2003 Chin. Phys. Soc.
and IOP Publishing Ltd

Calculation of scanning tunnelling microscopy images for Kr/graphite system*

Zhou Xiao-Lin(周晓林)[a)b)], Chen Xiang-Rong(陈向荣)[a)c)†],
Yang Xiang-Dong(杨向东)[a)b)], and Gou Qing-Quan(苟清泉)[a)]

[a)] *Institute of Atomic and Molecular Physics, Sichuan University, Chengdu* 610065, *China*
[b)] *Department of Physics, Sichuan Normal University, Chengdu* 610066, *China*
[c)] *Institute of Physics, University of Tsukuba,* 1-1-1 *Tennodai, Tsukuba* 305-8571, *Japan*

(Received 19 November 2002; revised manuscript received 14 April 2003)

The scanning-tunnelling-microscopy (STM) images of Kr atoms adsorbed on a monolayer graphite sheet (Kr/graphite system) are calculated using the first-principle total-energy electronic structure calculations within the density functional theory in the local density approximation. The results obtained agree well with the observations. It is found that the optimal site of the adsorbed Kr atom is at the top of the centre of the carbon hexagon, and its equilibrium distance from monolayer graphite surface is about 0.335nm. It is shown that the hybridization of C 2p electronic states (π-electronic states) and Kr 4p and 5s electronic states is the main origin of the Fermi-level local density of state.

Keywords: surface electronic states, local density approximation, scanning tunnelling microscopy, graphite
PACC: 7320A, 7320F, 7115M

The scanning tunnelling microscopy (STM)[1−3] provides us with a useful tool in surface physics for imaging of various adsorbate atoms and molecules on atomically flat surfaces at ultra-low temperatures and under ultra-high vacuum.[4−6] As an adsorbate, the rare gas atom has a long tradition in serving as a model system in surface physics due to its closed shell electronic structure and the weak interaction with the substrate. There have been a few STM observations of rare gas atoms adsorbed on metal and graphite surfaces so far. Eigler *et al*[7] have obtained images of individual Xe atom adsorbed on the Ni (110) surface. Grimm *et al*[5] have obtained STM images of Xe atoms on graphite surface. More recently, Matsui *et al*[8] have obtained the STM images of monolayer Kr and Xe atoms adsorbed on graphite surface. According to the theory of Tersoff and Hamann,[9] which shows that for a small bias voltage and constant current, a STM image (tunnelling current density) corresponds to a map of constant local density of state (LDOS) at Fermi level at the position of the tip, whether or not an adsorbate is visible in the STM experiment depends on how it modifies the LDOS near the Fermi level. The rare gas atoms adsorbed on the metal or graphite surface, however, are unlikely to modify the LDOS near $E_{\rm F}$ since the energies of the highest filled states of the rare gas atoms are much lower, and those of the lowest-lying empty states are much higher than $E_{\rm F}$. Thus, it was surprising that Kr and Xe atoms are visible in the STM experiments. Eigler *et al*[7] have used an atom-on-jellium model to interpret their STM images observed for the Xe/Ni (110) system. They have argued that the resonance of the empty Xe 6s state is the main origin of the Fermi-level LDOS, which makes Xe atom visible in the STM. How about Kr atoms adsorbed on metal and graphite surfaces? The origin has not been studied yet.

In this paper, we present the calculated STM images of a commensurate $(\sqrt{3}\times\sqrt{3})R30^\circ$ phase of Kr atoms adsorbed on the monolayer graphite sheet (Kr/graphite system).[10] All the work has been performed using first-principle total-energy electronic structure calculations within the density functional theory (DFT)[11,12] in the local density approximation

*Project supported by the National Natural Science Foundation of China (Grant No 10274055).
†Corresponding author. E-mail: chen@cm.ph.tsukuba.ac.jp

(LDA). The atom-adsorbed graphite surface is simulated by a repeating slab model, in which the graphite layers are separated substantially to avoid artificial interactions. For the exchange-correlation energy among electrons, we use a functional form[13] fitted to the Monte Carlo results for the homogeneous electron gas.[14] Norm-conserving pseudopotentials generated by using the Troullier–Martins scheme are adopted to describe the electron–ion interaction.[15,16] In constructing the pseudopotentials, core radii adopted are 1.50, 1.54 and 1.54a.u. for C 2s, 2p, and 3d states, respectively, and 1.80, 1.85 and 1.85a.u. for Kr 4s, 4p and 4d states, respectively. The valence wavefunctions are expanded by the plane-wave basis set with a cutoff energy of 50Ryd, which gives enough convergence of relative total energies of carbon-related system.[15] The conjugate-gradient minimization scheme is used both for the self-consistent electronic structure calculations and for the geometry optimization. Integration over the surface Brillouin zone is carried out using an $8k$-point sampling with one k-point in the z-direction in the self-consistent calculations. Detailed accounts for the calculation method have been also seen elsewhere.[17,18]

The equilibrium lattice constant of a $(\sqrt{3} \times \sqrt{3})R30^\circ$ monolayer graphite surface obtained is 7.961a.u. (0.4213nm) with an accuracy of 1.1% compared with the experimental value, 0.4260nm. And then, the full geometrical optimizations are performed for the commensurate $(\sqrt{3} \times \sqrt{3})R30^\circ$ phase of Kr atoms adsorbed on the graphite sheet to determine the optimal site for the adsorbed Kr atom and its distance from the graphite surface. Here, three different possible adsorption sites, i.e. the C (top of the centre of the carbon hexagon), B (top of the centre of the C–C bond), and T (top of a carbon atom) sites, have been considered. We find that the C site with the equilibrium distance of 0.335nm from the graphite surface is the most stable for the Kr adsorption. It is also found that the corresponding equilibrium distances from the graphite surface for the B and T sites are both 0.340nm. The differences in total energy are 7.4meV between the C and B sites and 8.0meV between the C and T sites. These small values indicate that the commensurate-incommensurate (CI) structural transition is easy to occur for Kr atoms adsorbed on graphite surface even at low temperatures. In this work, we only consider the C site at the equilibrium position.

In Fig.1, we show the calculated electronic band structure of the Kr/graphite system together with that of the $(\sqrt{3}\times\sqrt{3})R30^\circ$ monolayer graphite surface. It is obvious that the top of the valence bands and the bottom of the conduction bands for the Kr/graphite system and for the $(\sqrt{3}\times\sqrt{3})R30^\circ$ monolayer graphite surface are both at Γ point and the four energy bands of π-electrons are degenerate at Γ point, as is different from that of 1×1 monolayer graphite surface.[19] For 1×1 monolayer graphite surface, the degeneracy appears at K point, which is folded at Γ point in the $(\sqrt{3} \times \sqrt{3})R30^\circ$ periodicity.

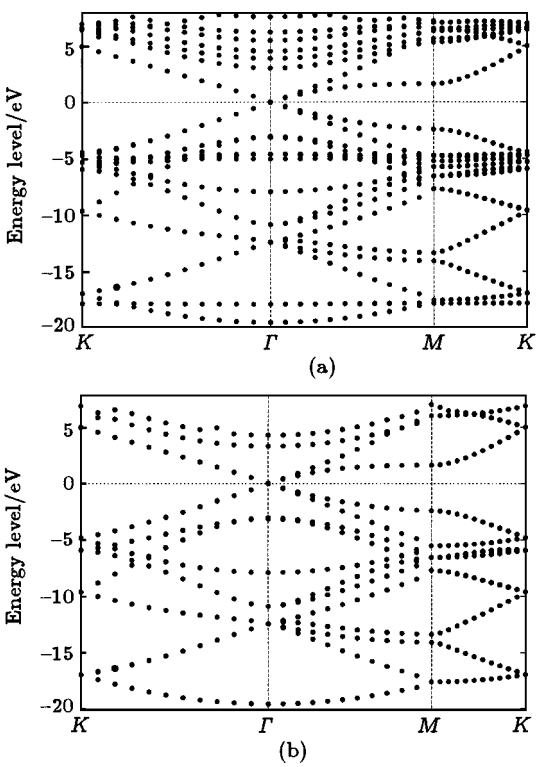


Fig.1. Calculated electronic band structures for: (a) Kr/graphite system, (b) $(\sqrt{3} \times \sqrt{3})R30^\circ$ monolayer graphite surface. Energy levels are relative to the Fermi level $E_{\rm F}$.

To calculate the STM images for the Kr/graphite system, we use the following expression for tunnelling current density,[20]

$$j_{\pm}(\boldsymbol{r}, V) = \pm \int_{E_{\rm F} \mp |V|}^{E_{\rm F}} \sum_{nk} |\psi_{nk}(\boldsymbol{r})|^2 \delta(E - E_{nk}) {\rm d}E, \quad (1)$$

where $\psi_{nk}(r)$ and E_{nk} represent the wavefunction and the corresponding eigenvalue for the state with the band index n and the wavenumber k, $\boldsymbol{r}$ is the position of the STM tip, and V is the applied bias voltage between the tip and the sample. The $\pm$ signs denote the

filled-state and empty-state STM images corresponding to the negative and positive sample bias voltage, respectively.

The calculations of STM images are performed using 99 k-points that sample the $\boldsymbol{k}$-space region near E_{F} in the rectangular area in Brillouin zone (see Fig.2(a)). The results obtained are shown in Figs 2(c)–(e). They are shown on a typical plane parallel to the graphite surface with the distance of 0.45nm (the height is 0.115nm above the adsorbed Kr atom). The schematic diagram (parallel to the graphite surface) of the Kr/graphite system is shown in Fig.2(b): the rhombus $ABCD$ denotes the unit cell; the rectangle $ABEF$ corresponds to the plane on which the STM images are shown; the solid and open circles denote the sites of Kr and C atoms, respectively. For these calculations, we take the spacing of two adjacent graphite sheets in the slab model as 1.80nm to avoid the interactions between graphite surfaces.

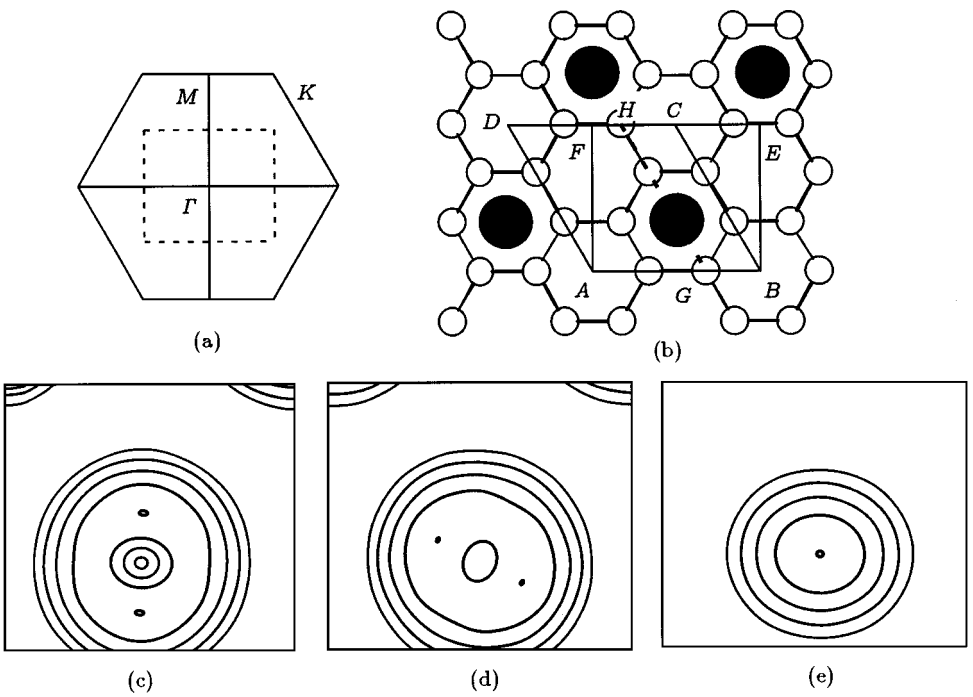


Fig.2. (a) The hexagonal Brillouin zone of the Kr/graphite system. The 99 K-points adopted for STM calculations is in the rectangular area near Γ point. (b) The schematic diagram of the Kr/graphite system, where the rhombus $ABCD$ denotes the unit cell. The rectangle $ABEF$ corresponds to the plane on which the STM images are shown. The solid and open circles denote the sites of Kr and C atoms, respectively. The calculated STM images (tunnelling current density) for the Kr/graphite system at the sample bias voltages of (c) V=–1eV, (d) V=1eV, and (e) V=2eV. The subsequent contours differ by a factor of 1.5.

In the filled-state image shown in Fig.2(c), we find that the brightest position in the tunnelling current density is located on the top of Kr atom forming elongated circles. On the other hand, in the empty-state image shown in Fig.2(d), the brightest position is also located on the top of Kr atom, but the elongated circles are along a different direction. As the positive bias voltage is increased from 1eV to 2eV, the elongated circles become regular circles. All these indicate that Kr 4p or/and 5s states contribute to the LDOS of the Kr/graphite system near E_{F}. In both positive and negative bias voltages, C atoms are not visible because of the large distance between the STM tip and the graphite surface. To clarify the origin of the images in Figs 2(c)–(e), we show the contour plots of the calculated LDOS on a plane normal to the graphite surface in Fig.3. We find that the filled states near E_{F} are mixed with p orbitals at the Kr site, whereas the empty states are with more s-like orbitals. This finding is consistent with the notion that the filled states are mixed with Kr 4p states, whereas Kr 4p and 5s states contribute to the empty states near E_{F}.

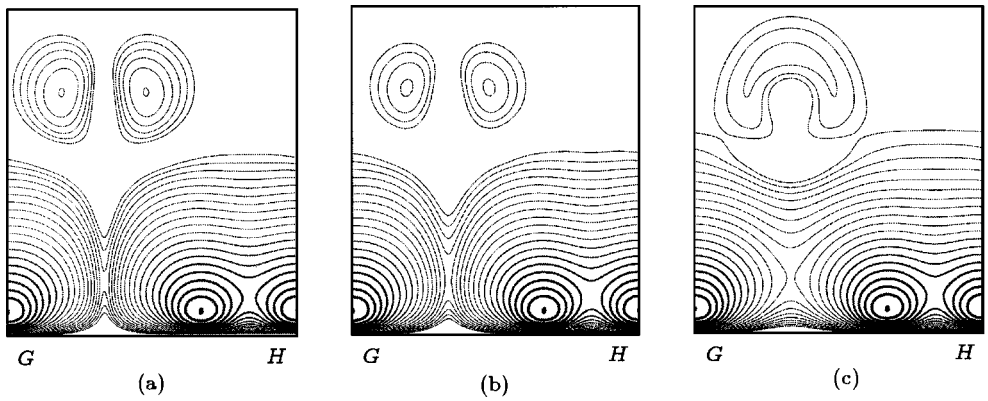


Fig.3. Contour plots of local density of state for the Kr/graphite system on a plane perpendicular to the graphite surface at the sample bias voltages of (a) V=−1eV, (b) V=1eV, and (c) V=2eV. The plane, the height of which is 0.45nm, includes the dashed line GH in Fig.2(b). The subsequent contours differ by a factor of 1.5.

It is seen clearly from Fig.1(a) that the electronic states of the Kr/graphite system near E_{F} consist mainly of the π-electronic states of graphite: two antibonding π-electronic states above E_{F} contribute to the empty-state STM images and two bonding π-electronic states below E_{F} contribute to the filled-state STM images. C 2s and Kr 4s electronic states are unlikely to contribute to the LDOS of the Kr/graphite system near E_{F} because they are deep in energy. To confirm that Kr 4p and 5s states contribute to the LDOS near E_{F}, we have examined the LDOS at Γ point in different energy regions: (a) −4.77eV (corresponding to Kr 4p states), (b) 3.04eV, (c) 3.90eV, and (d) 4.54eV ((b), (c), and (d) corresponding to the first, the second and the third conduction bands above E_{F}, respectively). Figure 4 shows the contour plots of the calculated LDOS on the rectangular plane normal to the graphite surface along the dashed line GH in Fig.2(b) near these energies below 5eV. From these results obtained, we speculate that C 2p electronic states and Kr 4p and 5s electronic states are mixed substantially in the energy region far from the Fermi level E_{F}. This means that the mixing also takes place near E_{F}. Hence, we conclude that the STM images of the Kr/graphite system are mainly due to the hybridization of C 2p electronic states (π-electronic states) with Kr 4p and 5s electronic states.

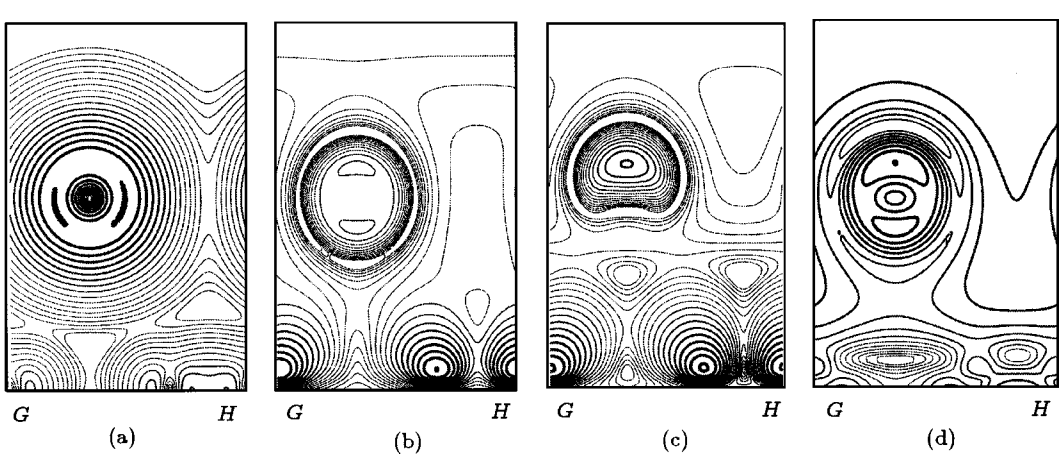


Fig.4. Contour plots of the local density of states for the Kr/graphite system on a plane perpendicular to the graphite surface corresponding to the energy regions: (a) from −5.07eV to −4.57eV; (b) from 2.98eV to 3.08eV; (c) from 3.85eV to 3.95eV, and (d) from 4.49eV to 4.59eV. The plane, the height of which is 0.6nm, includes the dashed line GH in Fig.2(b). The subsequent contours differ by a factor of 1.5.

Acknowledgments

The authors thank Professor H Fukuyama for his providing us the STM experimental data of Kr/graphite system. All calculations are performed using Fujitsu VPP5000 of Science Information Processing Centre in University of Tsukuba.

References

[1] Binnig G, Rohrer H, Gerber Ch and Weibel E 1982 *Appl. Phys. Lett.* **40** 178
[2] Binnig G, Rohrer H, Gerber Ch and Weibel E 1982 *Phys. Rev. Lett.* **49** 57
[3] Binnig G, Rohrer H, Gerber Ch and Weibel E 1983 *Phys. Rev. Lett.* **50** 120
[4] Pan S H, Hudson E W and Davis J C 1999 *Rev. Sci. Instrum.* **70** 1459
[5] Grimm B, Hövel H, Pollmann M and Reihl B 1999 *Phys. Rev. Lett.* **83** 991
[6] Over H, Seitsonen A P, Lundgren E, Schmid M and Varga P 2002 *Surf. Sci.* **515** 143
[7] Eigler D M, Weiss P S, Schweizer E K and Lang N D 1991 *Phys. Rev. Lett.* **66** 1189
[8] Matsui T, Kambara H and Fukuyama H 2002 *J. Low Temp. Phys.* **126** 373
[9] Tersoff J and Hamann D R 1983 *Phys. Rev. Lett.* **50** 1998 Tersoff J and Hamann D R 1985 *Phys. Rev.* B **31** 805
[10] The Kr monolayer tends to have a structure incommensurate to the periodicity of the graphite $(\sqrt{3} \times \sqrt{3})R30^\circ$ presumably due to the small atomic radius: Chinn M D and Fain S C Jr 1977 *Phys. Rev. Lett.* **39** 146. The long-range order of the monolayer rare gas atoms is not of our focus, however.
[11] Hohenberg P and Kohn W 1964 *Phys. Rev.* **136** B864
[12] Kohn W and Sham L J 1965 *Phys. Rev.* **140** A1133
[13] Perdew J P and Zunger A 1981 *Phys. Rev.* B **23** 5048
[14] Ceperley D M and Alder B J 1980 *Phys. Rev. Lett.* **45** 566
[15] Troullier N and Martins J L 1991 *Phys. Rev.* B **43** 1993
[16] Kleinman L and Bylander D M 1982 *Phys. Rev. Lett.* **48** 1425
[17] Oshiyama A 1995 *Phys. Rev. Lett.* **74** 130
[18] Okada S, Saito S and Oshiyama A 2002 *Phys. Rev.* B **65** 165410
[19] Chen X R, Oshiyama A, Okada S and Gou Q Q 2003 *Chin. Phys. Lett.* **20** 404
[20] Yu B D, Ide T and Oshiyama A 1994 *Phys. Rev.* B **50** 14631